Hydraulic and Civil Engineering Technology VII
M. Yang et al. (Eds.)

doi:10.3233/ATDE220909

Critical Speed of Subgrade with Arbitrary Complex Section: In Wave Excitation and Propagation View

Rui WANG [a,b], Xiang REN [b], Zhiping HU [b,1], Wei SHI [a] and Jiakuan MA[a]
[a] *Urban Geology and Underground Space Engineering Technology Research Center of Shaanxi Province, Xi'an 710061, China*
[b] *School of Civil Engineering, Chang'an University, Xi'an 710061, China*

Abstract. As the train speed increases, there are two typical dynamic response patterns of subgrade, i.e. with or without wave propagation. Once the wave propagation occurs, the track displacement begins to increase sharply and the environmental vibration becomes more and more significant. The determination of the critical speed at where waves are emitted is significant for relative investigation and engineering practice. To this end, the dynamic behaviors of a track-embankment-ground system in speed-frequency domain were discussed and a determination approach of the critical speed was proposed. To confirm the prediction ability, verifications were carried out on typical semi-infinite ground and track-embankment-pile reinforcement ground system. The results indicate that the phase plot performs satisfactory in predicting the critical speed of subgrade with arbitrary section. The appearance of phase shift reflects the intrinsic feature of energy dissipation with radiation of waves.

Keywords. Subgrade, wave excitation, phase shift, 2.5D finite element method

1. Introduction

Railway transportation occupies a pivotal position in modern transportation industry. The dynamic responses of subgrade subjected to moving train loading are of significance for the design, construction and operation of railway lines. As relative researches continue to be proposed, the dynamic response characteristics of the subgrade are gradually and clearly delineated.

Critical speed is frequently adopted to represent the critical dynamic state of subgrade under moving train loading [1-3], such as the appearance of maximum vertical displacement of track (critical speed I hereinafter) and the excitation of waves (critical speed II), as shown in figure 1. Madshus and Kaynia [1] have verified the existence of critical speed I through field measurement data and pointed out that wave excitation is a significant sign for the dynamic behavior of subgrade. Once the wave propagation occurs, the dynamic displacement begins to increase sharply and the environmental vibration becomes more and more significant.

[1] Zhiping Hu, Corresponding author, School of Civil Engineering, Chang'an University, 75 Middle Chang'an Road, Yanta District, Xi'an City, Shaanxi Province, China; E-mail: huzhping@chd.edu.cn.

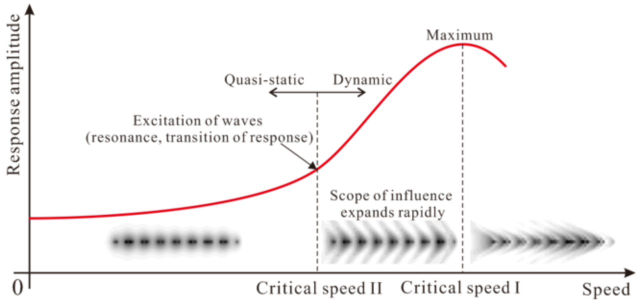

Figure 1. Diagram of the response state of subgrade under moving train loading.

The critical speed I is fully dominated by the properties of wave propagation in subgrade and of the bending wave propagation in the track. It is firstly studied through the theoretical solution of the beam structure resting on the half-space gound [4,5]. Recently, the finite element method is widely used to obtain the critical speed I of subgrade with complex section [6,7]. A significant trend of current work is to fit engineering practice as far as possible. Sayeed and Shahin [6] have analyzed the effects of soil layer stiffness, axle loading and train type on the critical speed. Hu et al. [8] have investigated the critical speed of ballastless track-embankment-soft ground system and introduced the effects of embankment on the dynamic stress in subgrade. Regarding to the prediction of the critical speed I, Dieterman and Metrikine [4] have pointed out that the resonance occurs when the loading speed is equal to the group velocity of the waves. Sheng et al. [9] have found that the critical speed I can be interpreted in terms of the dispersion characteristics of the track and ground combination. Inspired by Sheng et al. [9], Costa et al. [3,10] have proposed an efficient prediction approach of critical speed I referring the dispersion relationship of the subgrade and track.

The critical speed II is the bound of the quasi-static and dynamic responses of subgrade under moving loading [6]. It is not only significant for the assessment of dynamic response but also the modeling strategy of finite element. For example, the absorbing boundary might be not necessary when no wave emitted [11]. It is easily to determine the critical speed II of half-space ground, i.e. the Rayleigh wave velocity of ground [10,12]. However, section of the actual railway line generally cannot ideal half-space ground. The cutting, the embankment and the ground reinforcement measure are very common and necessary to take into account. The traditional dispersion spectra method is not able to determine the critical velocity of complex section foundation. To data, traversing dynamic responses of subgrade is the only way to confirm the critical speed II of subgrade with complex profile. Significant computational effort hinders detailed discussion and engineering application.

The present study goes into propose an efficient prediction approach of critical speed II of subgrade with arbitrary section. To this end, the 2.5D finite element method was utilized to obtain the dynamic responses of track-embankment-ground system. An efficient criterion is selected after referring Dieterman and Metrikine [12]. As further discussion, the effects of track irregularity on the wave excitation characteristic of subgrade were also addressed.

2. Theoretical background

The dispersion relation illustrated in the frequency-wave number (ω-ξ) domain is an appropriate selection to efficiently represent the dynamic characteristic of subgrade under variable train speed (v). The dynamic response in speed range from zero to infinity (0~∞) can be found in a single map of dispersion relation, with a relationship of $v=\omega/\xi$. A fast prediction method of the critical speed I is taking the intersection point of the ground and track dispersion curves as reference point, at where the wavelengths of the waves that propagate along the track and over the ground match well [3,10].

For subgrade with complex profile, the dispersion relation can be illustrated by solving the site-specific dynamic transfer function $\tilde{\bar{H}}(\omega,\xi)$ as follow [1,13]:

$$\tilde{\bar{R}}(\omega,\xi)=\tilde{\bar{H}}(\omega,\xi)\cdot\tilde{\bar{P}}(\omega,\xi) \tag{1}$$

where $\tilde{\bar{R}}(\omega,\xi)$ is the response function and $\tilde{\bar{P}}(\omega,\xi)$ refers to the train load excitation function. The functions $\bar{P}$ and $\tilde{P}$ represent the transformed load with respect to time and space.

In relative researches, vertical displacement of track is often selected to depict the dynamic response characteristic of system. Madshus and Kaynia [1] have suggested the critical speed I can be determined referring the coincidence between peaks in $\tilde{\bar{H}}(\omega,\xi)$ and $\tilde{\bar{P}}(\omega,\xi)$. In the subsequent discussion, the dynamic transfer function of vertical displacement of track is also adopted to analyze the dynamic features of system with or without wave propagation behavior.

In the present study, the 2.5D finite element method is utilized to obtain the dispersion relation of track. Due to space limitation, all the basic theory is not introduced. Reader can find any detail in relative references [14-16]. The accuracy of the self-compiled program is validated by a classical solution [17]. The model information can be found in Wang et al. [18]. Dynamic responses of a point 1.0 m beneath the loading line were obtained. The displacements normalized by multiplying $2\pi\rho c_s^2/F$ are shown in figure 2.

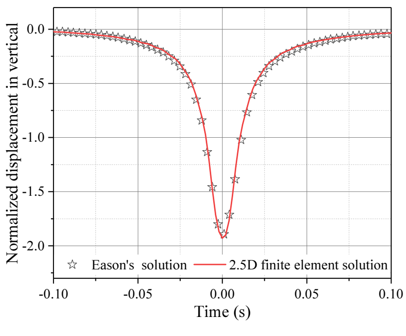

(a)

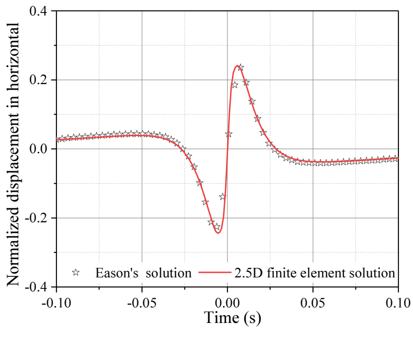

(b)

Figure 2. Displacement of the observation point in half-space foundation under moving point loading. (a) in vertical; (b) in horizontal.

3. Model Information

In order to fully illuminate the characteristic of subgrade with complex profile, a track-embankment-ground system as shown in figure 3 is adopted herein. This profile is generalized from the subgrade in loess region of Chine. A classical geologic profile of ground is selected. Soil parameters are listed in table 1.

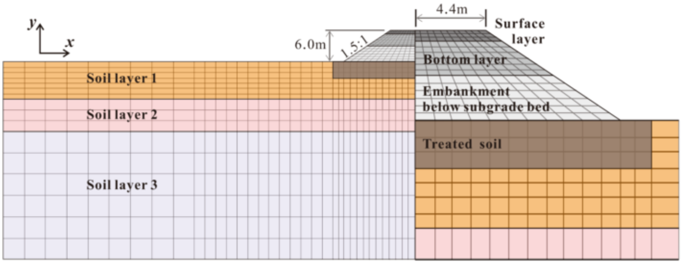

Figure 3. Outline and meshing of model cross section.

Table 1. Parameters of soil layer.

Soil layer	Number	Thickness /m	Density /kg·m^{-3}	Modulus /MPa	Damping ratio	Poisson's ratio
Surface layer of subgrade bed	1-1	0.7	1900	86.5	0.04	0.25
Bottom layer of subgrade bed	1-2	2.3	1900	96.0	0.04	0.25
Embankment below subgrade bed	1-3	-	1800	50.0	0.04	0.25
Treated soil	2	3.0	1800	50.0	0.04	0.3
Soil layer 1	3-1	7.0	1980	26.3	0.05	0.32
Soil layer 2	3-2	6.0	1880	17.9	0.05	0.33
Soil layer 3	3-3	24.0	1990	41.1	0.05	0.32

There are two generic choices of track structure type, i.e. ballasted and slab track. To data, the ballasted track contributes to more than 95% of railway system [19]. In many countries, the ballasted track is the main selection in high-speed railway, such as in France, Spain and Italy. Therefore, the ballasted track was selected herein. The track system was modeled as an Euler beam with a width of 4m and the parameters was assumed as bending rigidity EI=13.254MN·m^2 and mass per unit length m=540kg/m [16]. The viscoelastic dynamically artificial boundary was adopted to simulate the absorbing effect of outer domain. The geometrical parameter of CRH3 train with axle weight of 17t is shown in figure 4.

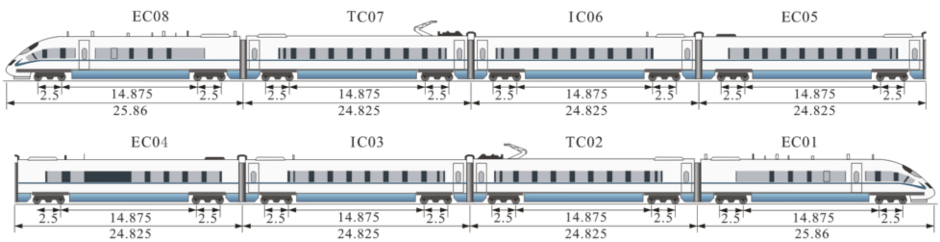

Figure 4. Relative axle position of the CRH3 train.

4. Results

The objective of the present study is to suggest an efficient approach to determine the critical speed II at where the wave propagation emerges. To this end, the vertical displacement contour plots around the critical speed II were obtained, as shown in figure 5. The Mach cone can be easily recognized from figure 5 with v=65 and 70m/s. Moreover, an obvious transition trend could be found, and it is reasonable to approximately take 60-65m/s as the critical speed II range of the model delineated in figure 3.

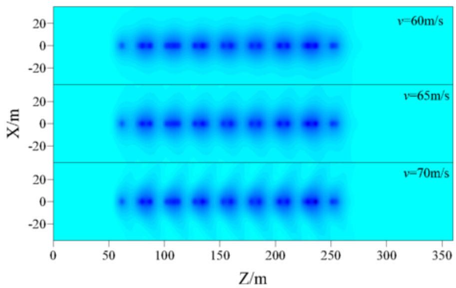

Figure 5. Vertical displacement contours on the surface with different train speeds near the critical speed II.

With regard to the criterion of response pattern change, it is still expected to be proposed by analyzing the dispersion relation. The dispersion relation (vertical displacement amplitude of track to unit vertical load, Ntotsios et al. [13] depicted in speed-frequency (v-f) domain is shown in figure 6. As can be seen from figure 6, the spectrum smoothly transform at lower velocity range (0~60m/s). With the continually increase of speed, a peak region emerges and change of spectrum signature becomes more and more evident. It is generally accepted that the dynamic displacement feature will change with the appearance of wave propagation. The interaction between adjacent axle loadings might change the curve shape of dynamic response [1]. Therefore, the lower boundary limit of the peak region might be taken as critical speed II at where the Mach effect occurs. That is an interpretation from the traditional view of dispersion relation. It is reasonable but the lower boundary limit of the peak region is always hard to be distinguished.

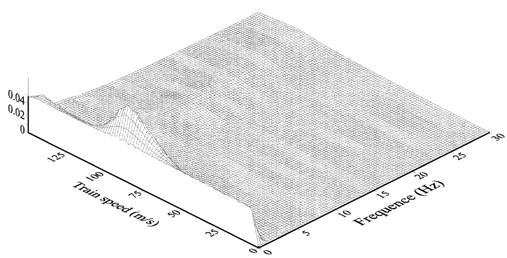

Figure 6. The amplitude varation of vertical displacement of track (dispersion relation).

Dieterman and Metrikine [12] have derived the equivalent stiffness of an elastic half-space with a finite width beam rested on. A conclusion has been drawn that the wave propagation is emitted once the phase velocity of the waves in the beam exceed the velocity of the Rayleigh waves in the half-space. In the meantime, the imaginary part of the equivalent stiffness is no longer equal to zero. That can be explained by the energy dissipation in system which is connected only with radiation of elastic waves.

Inspired in the above study, the phase of vertical displacement response of track to unit vertical loading was calculated and illustrated in figure 7, which has rarely been addressed in the previous study. An interesting trend can be evidently found that the phase remains about 3.14 rad (π) in a lower velocity range (0~62.5m/s), which is the range at where no wave propagation exists. The phase equals to π means that the response is a negative real number under unit loading. Once the speed exceeds critical speed II, about 62.5m/s, the phase begins to change rapidly. The imaginary part of response is no longer equal to zero. Actually, the 'out-of-phase' phenomenon in track displacement is already summarized long time ago, and makes the interaction between the adjacent bogie loadings as a significant factor when determining the critical speed I [1,6]. Thus, the phase shift can be utilized as efficient criterion of the change from quasi-static state to dynamic state.

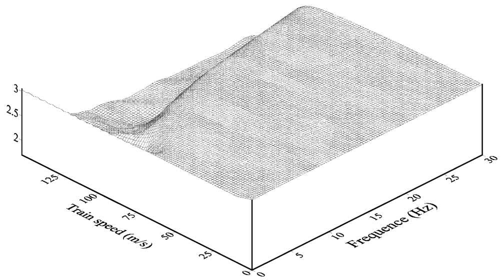

Figure 7. The phase varation of vertical displacement of track.

The shaded relief plots of figure 6 and figure 7 are shown in figure 8. A clear borderline can be delineated in figure 8 (b). Therefore, a conclusion can be drawn that using the phase depicted in speed-frequency (*v-f*) domain as the criterion of critical speed II can not only clearly reflect the nature of energy dissipation, but also have higher identification.

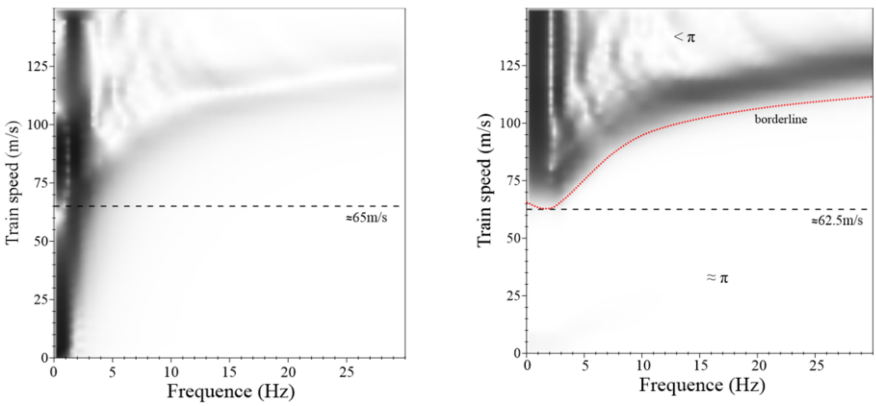

(a) (b)

Figure 8. The amplitude (a) and phase (b) plots of vertical displacement of track.

5. Verification

To further confirm the prediction ability of the phase plot depicted in speed-frequency (v-f) domain, a semi-infinity ground and a track-embankment-pile reinforcement ground system are adopted. Two typical pile reinforcement measures, i.e. the soil-cement compacted (SC) pile and the CFG pile, are selected to change the dynamic characteristic of subgrade with complex profile.

5.1. Semi-infinity Ground

The semi-infinity ground was approximated with a homogeneous soil stratum of 36m on the rigid bedrock, no track structure resting on. The density ρ is, shear-wave velocity c_s, Poisson's ratio υ and damping ratio η of the soil are 1600 kg/m^3, 90 m/s, 0.3 and 0.04, respectively. The Rayleigh wave velocity is about 83.5 m/s. It is well known that the critical speed of semi-infinite ground is equal to or slightly lower than Rayleigh wave velocity, when the ground can be assimilated to a homogeneous half-space [10]. The phase plot (figure 9) indicates a good agreement between the Rayleigh wave velocity line and border of the phase.

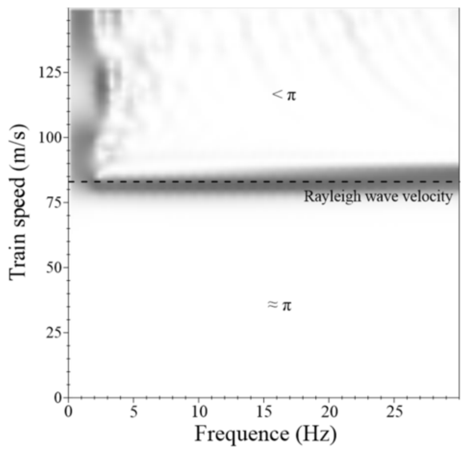

Figure 9. The phase plot of vertical displacement of semi-infinite ground.

5.2. Track-embankment-pile Reinforcement Ground System

The outline and meshing of pile reinforcement ground are shown in figure 10. A 0.5m diameter and 15m length of pile was selected with a center spacing of 2.0m. According to the relative reference, the pile-soil contact was simulated by binding constraint and the equivalent dynamic modulus method was used to achieve the modulus equivalent, see Eq. (2). Parameters of soil layers and structure parts are listed in table 2. All the other information is the same as the model depicted in figure 3.

$$E_{sp} = \frac{\pi D}{4l} E_p + \left(1 - \frac{\pi D}{4l}\right) E_s \tag{2}$$

where l refers to the pile center spacing, D is the diameter of pile, E is the dynamic modulus, and subscripts sp, p and s refer to the equivalent pile wall, pile and soil among piles, respectively.

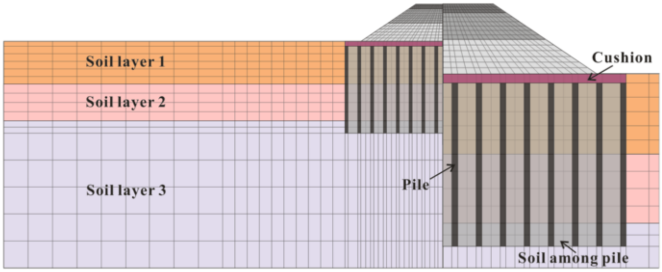

Figure 10. Outline and meshing of subgrade with pile reinforcement ground.

Table 2. Parameters of soil layer.

Soil layer or structure	Applicable model	Thickness /m	Length /m	Density /kg·m^{-3}	Modulus /MPa	Damping ratio	Poisson's ratio
Cushion	SC and CFG	0.8	\	2000	200	0	0.3
Soil-cement compacted pile	SC	\	15	2000	100	0	0.23
Soil among soil-cement compacted piles	SC	15	\	2000	50.0	0.04	0.25
CFG pile	CFG	\	15	2500	25500	0	0.17

The phase plots of vertical displacement response of track for the SC model and the CFG model are shown in figure 11. Critical speed II can be obtained referring the border of the phase plot, about 80 m/s and 108m/s for the SC model and the CFG model, respectively. Compared with the vertical displacement contour plots of these two models (figure 12), the Mach cone arises after the critical speed II. That is, the phase plot depicted in speed-frequency (v-f) domain performs satisfactory in predicting the critical speed II, at where the wave propagation begins to arise. This approach is suitable for the subgrade with arbitrary section, since the phase shift reflects the intrinsic feature of energy dissipation with radiation of waves.

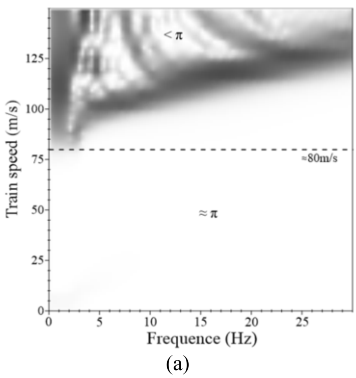

(a)

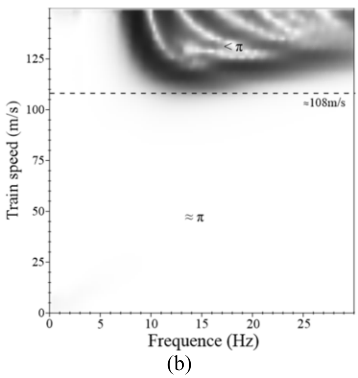

(b)

Figure 11. The phase plot of vertical displacement. (a) the SC model, (b) the CFG model.

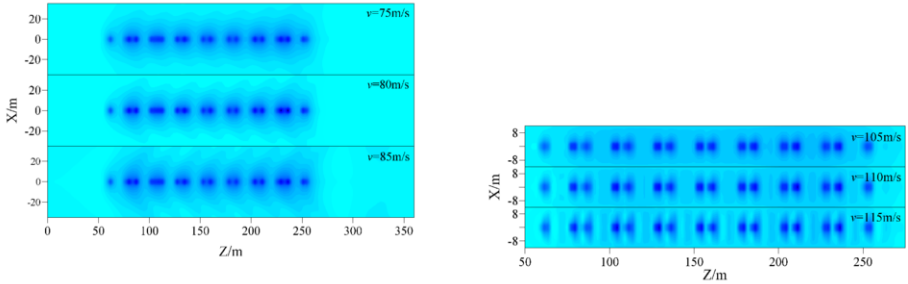

Figure 12. Vertical displacement contours on the surface with different train speeds near the critical speed II. (a) the SC model, (b) the CFG model.

6. Conclusions

The dynamic response of subgrade shows up two typical patterns, i.e. with or without wave propagation, as the moving train speed increases. The determination of the critical speed II, at where waves are emitted, is of significance for relative investigation and engineering practice. To this end, the performance of phase plot of vertical displacement depicted in speed-frequency (*v-f*) domain in predicting the wave propagation behavior has been studied. The results indicate that the phase plot performs satisfactory in predicting the critical speed II at where the wave propagation begins to arise. The appearance of phase shift reflects the intrinsic feature of energy dissipation with radiation of waves.

Acknowledgements

This work was supported by the Fundamental Research Funds for the Central Universities of China (Grant No. 300102281102) and the Open Research of Urban Geology and Underground Space Engineering Technology Research Center of Shaanxi Province (Grant No. 2022KT-02).

References

[1] Madshus C, Kaynia AM. High-speed railway lines on soft ground: dynamic behaviour at critical train speed. Journal of Sound and Vibration. 2000; 231(3): 689-701.

[2] Gao Y., Huang H, Ho CL, Hyslip JP. High speed railway track dynamic behavior near critical speed. Soil Dynamics and Earthquake Engineering. 2017; 101: 285-94.

[3] Costa PA, Soares P, Colaço A, Lopes P, Connolly D. Railway Critical speed assessment: a simple experimental-analytical approach. Soil Dynamics and Earthquake Engineering. 2020;134.

[4] Dieterman HA, Metrikine A. Critical velocities of a harmonic load moving uniformly along an elastic layer. Journal of Applied Mechanics. 1997;64(3):596-600.

[5] Picoux B, Le Houedec D. Diagnosis and prediction of vibration from railway trains. Soil Dynamics and Earthquake Engineering. 2005; 25(12): 905-21.

[6] Sayeed MA, Shahin MA. Three-dimensional numerical modelling of ballasted railway track foundations for high-speed trains with special reference to critical speed. Transportation Geotechnics. 2016; 6: 55-65.

[7] Yang JQ, Cui ZD. Influences of train speed on permanent deformation of saturated soft soil under partial drainage conditions. Soil Dynamics and Earthquake Engineering. 2020; 133.
[8] Hu J, Bian XC, Xu WC, Thompson D. Investigation into the critical speed of ballastless track. Transportation Geotechnics. 2019; 18:142-48.
[9] Sheng X, Jones CJC, Thompson DJ. A theoretical study on the influence of the track on train-induced ground vibration. Journal of Sound and Vibration. 2004; 272(3-5): 909-936.
[10] Costa PA, Colaço A, Calçada R, Cardoso AS. Critical speed of railway tracks. Detailed and simplified approaches. Transportation Geotechnics. 2015; 2:30-46.
[11] Shih JY, Thompson DJ, Zervos A. The effect of boundary conditions, model size and damping models in the finite element modelling of a moving load on a track/ground system. Soil Dynamics and Earthquake Engineering. 2016; 89: 12-27.
[12] Dieterman HA, Metrikine A. The equivalent stiffness of a half-space interacting with a beam. Critical velocities of a moving load along the beam. European Journal of Mechanics A/Solids. 1996;15(1): 67-90.
[13] Ntotsios E. Thompson DJ, Hussein MF. A comparison of ground vibration due to ballasted and slab tracks Transportation Geotechnics. 2019; 21.
[14] Yang YB, Hung HH. A 2.5 D finite/infinite element approach for modelling visco-elastic bodies subjected to moving loads. International Journal for Numerical Methods in Engineering. 2001; 51(11): 1317-36
[15] Takemiya H. Simulation of track–ground vibrations due to a high-speed train: the case of x-2000 at ledsgard. Journal of Sound and Vibration. 2003; 261(3): 503-26.
[16] Bian XC, Jing H, Thompson D, Powrie W. Pore pressure generation in a poro-elastic soil under moving train loads. Soil Dynamics and Earthquake Engineering. 2019; 125.
[17] Eason G. The stresses produced in a semi-infinite solid by a moving surface force. International Journal of Engineering Science. 1965; 2(6):581-609.
[18] Wang R, Hu ZP, Ma JK, Ren X, Li FT, Zhang F. Dynamic response and long-term settlement of a compacted loess embankment under moving train loading. KSCE Journal of Civil Engineering. 2021; 25(11): 4075-87.
[19] Jing GQ, Ding D, Liu X. High-speed railway ballast flight mechanism analysis and risk management – a literature review. Construction and Building Materials. 2019; 223: 629-42.